PHYSICAL REVIEW B **70**, 235208 (2004)

Interstitial nitrogen and its complexes in diamond

J. P. Goss, P. R. Briddon, and S. Papagiannidis
School of Natural Sciences, University of Newcastle upon Tyne, Newcastle upon Tyne, NE1 7RU, United Kingdom

R. Jones
School of Physics, The University of Exeter, Exeter EX4 4QL, United Kingdom

(Received 3 September 2004; published 17 December 2004)

Nitrogen, a common impurity in diamond, can be displaced into an interstitial location by irradiation. The resultant interstitial defects are believed to be responsible for a range of infrared and electronic transitions that vary in thermal stability, and on the type of diamond. Of particular prominence, and the only center for which an atomistic model has been suggested, is the *H*1*a* infrared band, which has previously been correlated with the vibration of isolated, bond-centered interstitial N. We present the results of a local-density-functional investigation of interstitial N and a range of complexes made up from N and self-interstitials. We disagree with the previous assignment of *H*1*a* to bond-centered interstitial N as we find it is not the ground state structure and it is mobile at temperatures at which *H*1*a* is stable. Instead we assign *H*1*a* to a complex of two N atoms sharing a single site in a [001]-split configuration, which is both more stable than isolated interstitial N and can simultaneously explain the infrared absorption and dependence on the aggregation stage of N in the irradiated material. We also make tentative assignments for other optical systems thought to involve interstitial N, and suggest schemes for hierarchical formation of complexes for Ia and Ib material.

DOI: 10.1103/PhysRevB.70.235208 PACS number(s): 61.72.Ji, 61.72.Bb, 71.20.Mq, 71.23.An

I. INTRODUCTION

Nitrogen content forms a cornerstone of diamond classification: diamond is termed “type I” if it contains significant concentrations, and “type II” otherwise. Type-I material is further subdivided into Ia and Ib depending on whether N is aggregated or in isolated substitutional centers (N_s), respectively. *A* centers (nearest-neighbor N pairs) and *B* centers (vacancies surrounded by four N atoms) represent the most common forms of N aggregates.

Ib material can be transformed to Ia by an appropriate high-temperature treatment: the activation energy for *A*-center formation is 4.8–6.2 eV (Refs. 1 and 2) with that for the formation of *B* centers being higher still.[1] Such high energies are indicative of the barrier to the interchange of nearest neighbors on the diamond lattice. However, the nitrogen diffusion rate depends on factors such as the annealing cycle[3] and applied pressure,[2] implying that the motion of N through diamond involves rather complex atomic processes. In particular, the interaction of native defects such as vacancies (V) and self-interstitials (I) changes the diffusivity of impurities,[3] with the mobility of N_s thought to be enhanced by a catalytic reaction with V.[4] Migration barriers for V and I, measured at 2.3 ± 0.3 eV (Ref. 5) and 1.7 eV (Ref. 6), respectively, are much lower than those for the formation of N aggregates.

There has been a focus on complexes of N with lattice vacancies, and assignment of a range of complexes to optical transitions, such as those from the NV complex at 1.945 and 2.516 eV,[7–9] and those labeled N2, N3, N4, H2, H3, and H4.[7,10–15] These optical centers, as with N_s and *A* and *B* centers, are stable to relatively high temperature. However, irradiation of diamond also produces mobile self-interstitials, even at cryogenic temperatures.[16] Self-interstitials contain short bonds and give rise to local-vibrational modes (LVM’s), as well as introducing states into the band gap.[17] Where N-containing material has been irradiated, both electronic and vibrational characteristics of interstitial-nitrogen defects are observed, but the structures of the defects responsible for these observations largely remain to be understood. It is the aim of this study to assign possible defect structures to these experimental observations, and we therefore briefly review selected data.

A. The *H*1*a* infrared absorption center

The *H*1*a* infrared (ir) center has been assigned to interstitial nitrogen (N_i).[18] *H*1*a* splits into three peaks with mixed $^{12}C/^{13}C$ (1450.0–1450.6, 1437.9–1438.9, and 1424.1–1425.1 cm^{-1}, depending on the ^{13}C concentration), indicating two equivalent C sites.[18] There is a 24 cm^{-1} shift with the N isotope, and two peaks in material with mixed N isotopes suggests only one N atom is involved.[19]

Subsequent to irradiation, *H*1*a* forms at 300 and 650 °C in Ia and Ib material, respectively. It is stable to around 1400 °C,[18] but whether this pertains to the diffusion of *H*1*a*, its dissociation, or the motion of a second defect to *H*1*a*, is not clear.

The difference between Ia and Ib materials is suggestive of a charge-state effect. Previous calculations suggest N_i adopts a puckered bond-centered configuration [Fig. 1(c)].[18,20] This was found to have vibrational modes broadly consistent with experiment, and this model has been widely accepted. The material-type dependence was explained by a barrier for the negative charge state to form N_i from a *more stable* N_s-I complex. However, the stability of *H*1*a* up to around 1700 K is inconsistent with the bridge-bonded structure, which has a *calculated* activation energy for diffusion

1098-0121/2004/70(23)/235208(15)/$22.50 ©2004 The American Physical Society

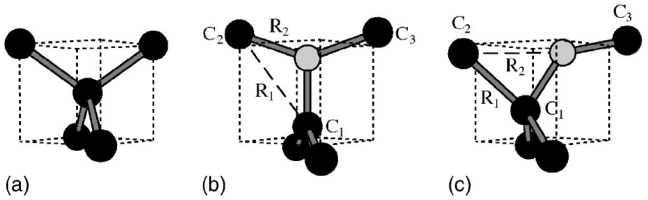

FIG. 1. The (b) [001]-oriented split-interstitial and (c) bond-centered configurations of N_i. Black and gray circles represent C and N, respectively. (a) shows the corresponding section of defect-free diamond for comparison, and the dashed lines indicate the cubic axes.

of $\leqslant 1$ eV,[18,21] much less than that of I, which diffuses thermally at around 700 K.[6]

Assuming N_i *is* responsible for *H*1*a*, the reactions

$$I + A \text{ center} \rightarrow N_s + N_i, \tag{1}$$

$$I + N_s \rightarrow N_i, \tag{2}$$

represent likely *H*1*a* production paths for Ia and Ib material, respectively.[18] However, Eq. (1) implies that N_i is mobile at 300 °C (the production temperature in Ia material) so that the N_s and N_i components can become spatially separated, which is inconsistent with the subsequent stability of *H*1*a* up to 1400 °C . We shall show later that this is resolved by correlating *H*1*a* with a more stable defect.

Finally, we note that in Ia material the concentration of *H*1*a* correlates with that of *A* centers, but is unrelated to that of *B* centers.[18] However, until now a direct role for *A* centers has not been suggested.

B. Other infrared-absorption centers

Other ir bands have been ascribed to interstitial nitrogen. One at 1502.0 cm^{-1} anneals out between 720 and 900 °C , shifts to 1479 cm^{-1} with ^{15}N, and might arise from a different charge state of the *H*1*a* center.[22] A peak at 1706 cm^{-1} also appears to arise from a defect containing a single nitrogen atom, and shifts by 28 cm^{-1} to lower frequency with ^{15}N.[23] This system, seen in material containing aggregated nitrogen, anneals in around 600 °C and out between 900 and 1400 °C.[23]

Finally, the 1856 cm^{-1} line exhibits a *three*-peak structure in material containing mixed nitrogen isotopes,[24] lying at 1856, 1833, and 1820 cm^{-1}. This defect, interpreted as containing two *equivalent* N atoms, is produced in irradiated Ia material subsequent to annealing, with thresholds at 500 and 900 °C.[24] In irradiated synthetic (Ib) material the line can be produced by annealing to 1400 °C, perhaps due to the formation of *A* centers,[24] suggesting that the 1856 cm^{-1} system is stable above this temperature.

C. N_i-related optical absorption and luminescence

Optical absorption bands correlated with N_i in irradiated Ib material lie at 2.367 and 2.535 eV, stable up to 200 and 400 °C, respectively. The 2.367 eV transition arises from a thermally populated state, and is frozen out at low temperature.[25] The absorption is bleached under suitable illumination, with a transition at 1.979 eV taking its place. It is suggested that the 2.367 and 1.979 eV transitions arise from different structural configurations of the same defect, with an activation energy for conversion of ~0.7 eV. Under annealing the 2.367 eV center may convert into the 2.535 eV center, possibly involving self-interstitial emission, leading to the suggestion that the former center contains at least two self-interstitials.[25] However, there is no direct evidence for the number of interstitial components to any of these optical absorption centers.

After annealing at 300–800 °C, cathodoluminescence (CL) peaks at 2.807 and 3.188 eV grow in intensity, although they are already present immediately after room-temperature electron irradiation.[24,26] The CL increases in intensity under the electron beam,[26] which may be interpreted as a change in charge state. Both CL bands anneal out at around the same temperature as *H*1*a*,[27] although to our knowledge, no formal correlation has been made between any of these centers.

The CL bands exhibit LVM replica. These lie at 1357, 1375, 1426, 1442, 1478, and 1536 cm^{-1} for the 3.188 eV center and at 1356, 1378, 1390, 1411, 1425, 1539, and 1602 cm^{-1} for the 2.807 eV center.[24,26] In material containing mixed nitrogen isotopes, several phonon replica split into two components, interpreted as the presence of a single N atom in the defect.[26]

It is generally taken that only totally symmetric modes couple to zero-phonon transitions. Under such an assumption it seems likely that the CL centers possess very low symmetry and/or contain several defect atoms: if the defect has high symmetry, in general only a subset of the normal modes will transform appropriately, meaning that there are more than seven LVM’s, whereas *I* is predicted to have three[28] or four[17] local modes, only one of which is totally symmetric. However, two coupled self-interstitials with no symmetry could potentially generate the seven one-phonon replica reported for the 2.807 eV system, suggesting that the CL systems may be multi-interstitial complexes.

In an attempt to determine the likely structures of the defects giving rise to the infrared bands and optical activity, we have examined the structure of N_i and complexes formed by the interaction of self-interstitials with N defects using first-principles simulations. We outline our method in Sec. II and present our results in Sec. III.

II. COMPUTATIONAL METHOD

Calculations were carried out using the local-spin-density-functional technique, implemented in ab initio modeling program[29] (AIMPRO). To model the various defects, 64–216-atom supercells have been used. The Brillouin zone is sampled using the Monkhorst-Pack scheme,[30] generally with a mesh of $2\times2\times2$ special *k* points. For representative cases we have compared total energies with a $4\times4\times4$ mesh, and this suggests our results from the smaller mesh are converged to of the order of 10 meV. Core electrons are eliminated by using norm-conserving pseudopotentials.[31]

The wave function basis consists of independent sets of *s* and *p* Gaussian orbitals with four different exponents, sited

TABLE I. Total energies (eV) for N_i in diamond relative to the [001] split-interstitial structure.

Model	Symmetry	Charge State -1	 0	 $+1$
Puckered bond center	C_s	0.3	1.2	1.7
Puckered bond center	C_2	0.3	1.3	1.9
Bond centered	D_{3d}	1.2	1.9	2.1
H site	D_{3d}	8.9	8.3	6.2
T site	T_d	11.0	11.2	10.0

at each C or N site. For C (N) 1 (4) additional atom-centered *d* Gaussians were also used. The charge density is Fourier transformed using plane waves with a cutoff of 300 Ry, which yields total energies converged to around 1 meV. The lattice constant and bulk modulus of diamond using these bases are within ~1 and 5%, respectively, of the experimental values, while the direct and indirect band gaps at 5.68 and 4.18 eV, respectively, are close to previously published plane-wave local-density approximation (LDA) values.[32]

Donor or acceptor electrical levels are estimated by comparison of the ionization potential or electron affinity of a bulk supercell, as suggested previously,[33] and discussed in detail for application to defects in diamond.[34] Vibrational modes are calculated by obtaining second derivatives of the total energy with respect to the atom positions for a subset of atoms (typically the defect atoms and their immediate neighbors). The dynamical matrix is then made up from a combination of these explicitly calculated terms and ones obtained from a valence force potential for the remaining atoms. Finally, we use the convention that a positive binding energy implies the reaction $A+B \rightarrow AB$ is exothermic.

III. RESULTS

A. Interstitial nitrogen, N_i

We have examined a number of likely configurations for N_i. The relative total energies are summarized in Table I. The N atom was displaced along $[11\bar{2}]$ or $[1\bar{1}0]$ from the [111] bond axis to generate puckered bond-centered structures with C_s and C_2 symmetry, respectively. Both relaxed defects have ∠CNC angles of ~135°, and C—N bond lengths of 1.26 Å. Previous, more approximate molecular-orbital calculations obtained a bond angle of 115° and C—N bond length of 1.47 Å.[18]

We find that the [001]-oriented split-interstitial structure is *significantly* more stable than any other configuration considered, and in particular 1.2 eV lower in energy than the puckered bond-centered geometry. The *T* and *H* interstitial sites are only viable when constrained by symmetry, and very high energy, whereas Kiflawi *et al.* found the hexagonal interstitial just 0.9 eV above the puckered bond center.[18]

The relaxed structures of the [001]-oriented split-interstitial and puckered bond-centered structured are shown in Figs. 1(b) and 1(c). The N—C bond lengths for the [001]-oriented split-interstitial structure are 1.37, 1.37, and 1.26 Å in the neutral structure, and differ from these values by just ±0.01 Å when charged. These, along with ∠CNC at 109° and 142° are within around 2% of those calculated for *I*, which is also a [001]-oriented split interstitial.[17,28,35]

We estimate the binding energy of $N_{i,\,[001]}$ relative to neutral N_s and *I* to be 5.6 eV, which represents the energy liberated in Eq. (2), and hence a considerable barrier to the reverse process. The large value results from the loss of two "dangling bonds"[36] (DB's) and suggests that once formed, $N_{i,[001]}$ will persist until it becomes mobile or complexes with another defect.

Following Ref. 18, we considered complexes made up from N_s and *I*. We find structures consisting of N_s with a self-interstitial at the *T* or *H* sites are unstable, and relax to the structure Fig. 1(b) or N_s-*I* pairs with *I* in a [001]-split configuration. However, this latter class of complexes may be important. There are many distinct N_s-*I* complexes. Four are shown schematically in Fig. 2, where the center of *I* is first, second, and third neighbor to N_s. Structures (a)–(c) have total energies 4.0, 3.6, and 2.4 eV above the ground-state structure [Fig. 1(b)]. Reorienting *I* in structure (c) produces (d), lowers the symmetry, and increases the total energy to 3.0 eV above the ground state. We find reorientation of the second-neighbor structure does not lead to reconstruction, and increases the total energy to around 4.3 eV. Separation to fourth neighbors increases the total energy to more

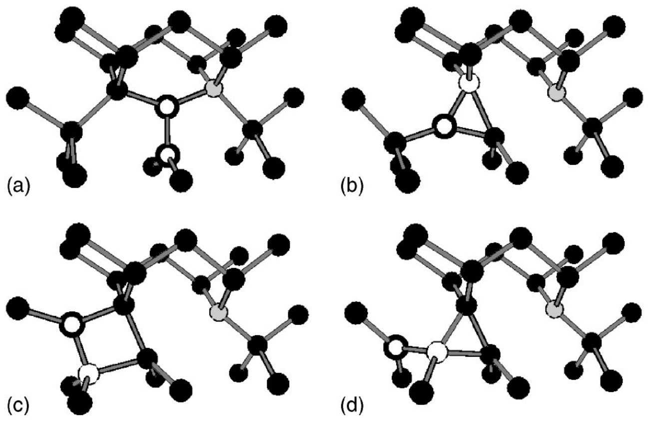

FIG. 2. Schematic representation of N_s and *I* in (a) nearest-neighbor, (b) next-nearest-neighbor, and (c) and (d) third-neighbor sites with different orientations. Circle shading as in Fig. 1, with the addition of white circles highlighting the C atoms in the split interstitial in each case. Threefold coordinated C atoms are indicated with the heavy black circles. The vertical and horizontal axes are approximately [001] and [110], respectively.

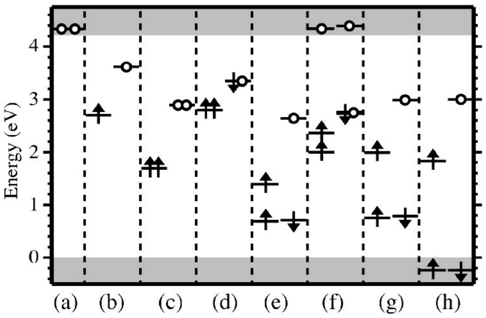

FIG. 3. Kohn-Sham eigenvalues in the vicinity of the band gap for N_i-related defects. (a) N_s^+, (b) N_s^0, (c) I, (d) I^-, (e) [001]-oriented N_i, (f) N_s neighboring I, (g) N_s and I second neighbors, and (h) N_s and I third neighbors. The valence-band top is at 0 eV, and the gray-shaded areas represent bulk bands. Arrows indicate occupied levels and their spin and white circles indicate empty levels. The calculated band gap of 4.2 eV is typical of the method.

than 5 eV above the ground state, which we interpret as the two components being effectively dissociated. Other configurations exist where N_s and I are at second or third neighbors, but which do not reconstruct and are relatively high in energy. We therefore conclude that the second- and third-neighbor pairs shown in Figs. 2(b)–2(d) represent the most significant metastable structures.

This result can be understood simply by counting the carbon DB's in each case. Recall that there is only a single DB in the case of $\mathrm{N}_{i,[001]}$. Where N_s borders I [Fig. 2(a)], it becomes on-site N_s^+, donating an electron to one of the the threefold-coordinated carbon atoms. However, this complex retains the two DB's of I. Where N_s is more distant from I, one N—C bond is broken and two threefold-coordinated C atoms then reconstruct to form a π bond, leaving N_s threefold coordinated with a filled lone pair. The resulting complexes have three- and four-member carbon rings, and only one DB.

The temperature to which one might expect the metastable forms to persist is difficult to estimate without an exhaustive analysis of the energy surface joining the various structures. However, qualitatively, the barrier to formation of from the third-neighbor pair must reflect the motion of the self-interstitial plus the breaking of the reconstruction, and is therefore likely to exceed the barrier for I migration.

1. *Electronic structure*

We find that $\mathrm{N}_{i,[001]}$ possesses a pair of levels in the band gap [Fig. 3(e)] with b_1 and b_2 symmetries in the C_{2v} point group. Electric-dipole transitions are forbidden between these levels, rendering the defect optically inactive. The lower band is mainly a filled lone pair localized on N. The higher band is partially filled in the neutral charge state, and is chiefly a p orbital on C_1 [Fig. 1(b)].

In the neutral charge state, N_i would be an orthorhombic $S=1/2$ paramagnetic defect, with the majority of spin density localized on carbon atoms: Mulliken population analysis suggests 1.5% and 56% of the spin density is localized on N and C_1, respectively. The defect is similar to I^-, although here the equivalence of the central atoms renders the p orbitals degenerate [Fig. 3(d)]. The gap levels of $\mathrm{N}_{i,[001]}$ are lower in the gap than those of N_s, I, and I^-, consistent with the binding energy relative to these components.

The $(-/0)$ and $(0/+)$ levels of N_i calculated using the comparison of ionization energies outlined in Sec. II lie at $E_c-1.6$ eV and $E_v+1.6$ eV, respectively, broadly in line with the Kohn-Sham spectrum, Fig. 3(e). In particular the $(-/0)$ level is close to the experimental donor level of N_s [$E_c-1.7$ eV (Ref. 37)]. Additionally, the highest occupied N_s^0 Kohn-Sham level is marginally above the lowest empty level of N_i [Figs. 3(b) and 3(e)], suggesting that N_s might donate an electron to N_i. Where N_s and N_i are at fourth-neighbor sites, charge transfer has occurred. This suggests that N_i may be negatively charged in Ib material, rendering it diamagnetic.

Also plotted in Figs. 3(f)–3(h) are the Kohn-Sham spectra of the metastable N_s-I complexes. The lower symmetry of these species (Fig. 2) render optical transitions dipole allowed, with the Kohn-Sham levels indicating zero-phonon energies around half the band gap, consistent with a tentative assignment of the 2.367 and/or 2.535 eV absorption centers to N_s-I complexes. The conversion of the former into the latter at 200 °C might correspond to the movement of I into a more stable configuration. Furthermore, the 2.367 eV arises from a thermally populated state, reminiscent of the complex optical characteristics of I.[17,38–40]

The electronic structures of the second- and third-neighbor pairs [Figs. 3(g) and 3(h)] resemble that of N_i since they also consist of a filled N lone pair and a single C-related DB. The relaxation in the third-neighbor pair is more extensive than the second, which results in a more stable lone pair lying around the top of the valence band.

2. *Migration of* N_i

Since *H*1*a* center is much more thermally stable than I, it is important to estimate the barrier to diffusion. We calculate this barrier assuming the path follows a

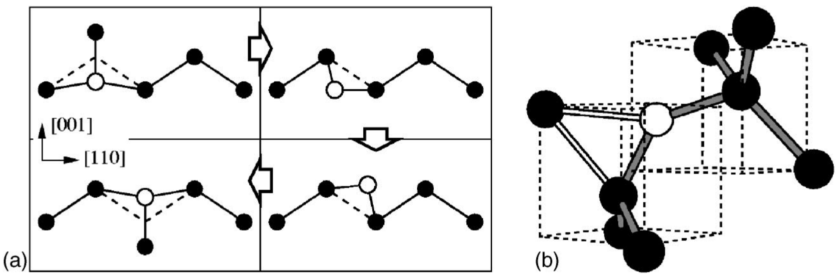

FIG. 4. (a) suggested trajectory for N_i in diamond. Black and white circles represent C and N, respectively. (b) is the saddle point structure.

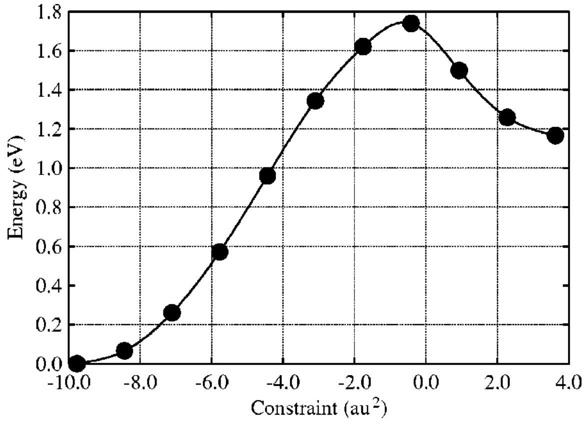

FIG. 5. Barrier to convert Fig. 1(b) into Fig. 1(c). The x axis is the constraint as discussed in the text. The computed data are indicated by black circles. The line joining the data is to guide the eye.

$$[001]\ \text{split} \rightarrow \text{bond center} \rightarrow [00\bar{1}]\ \text{split}$$

pattern, with the stages illustrated schematically in Fig. 4(a). This is the migration path predicted for N_i in silicon.[41] In this scheme the N atom moves, but note that the initial C component of the split interstitial does not.

The barrier height is estimated using a constrained minimization technique: differences in the squares of interatomic distances are fixed and all atoms allowed to relax subject to this constraint. For N_i we have $R_1^2-R_2^2=\text{const}$, where R_1 and R_2 are as indicated in Figs. 1(b) and 1(c). The energy profile as a function of the constraint is shown in Fig. 5, yielding a barrier of 1.7 eV. This step represents the barrier to migration provided the barrier to precession of the bond-centered configuration is less than the reverse $N_{i,[001]}$ to $N_{i,\text{BC}}$ reaction. Since we find that the barrier to precession is of the order of 0.1 eV, the activation energy in Fig. 5 represents that required to migrate N_i through the lattice. The saddle-point structure is shown in Fig. 4(b).

The migration barriers for the positive and negative charge states computed using the same method are estimated to be 2.4 and 0.8 eV, respectively. The difference with charge state reflects the changes in the relative stabilities of $N_{i,[001]}$ and $N_{i,\text{BC}}$ (Table I).

As previously noted, the partially dissociated pairs will possess a barrier to recombination. In particular, if Eq. (2) proceeds via structures in Fig. 2, there will be a barrier of 1.7 eV (the migration of I) plus the barrier to convert N_s-I into N_i. We have not calculated these barrier heights, but it seems plausible that conversion of Fig. 2(c) into Fig. 2(b), or indeed Fig. 2(b) into Fig. 2(a), might correspond to the 650 °C required for the formation of *H*1*a* in Ib material.

3. Local vibrational modes

LVM's constitute a key to obtaining an unambiguous identification for *H*1*a*. Those calculated for $N_{i,[001]}$ are listed in Table II, all of which are both ir and Raman active by symmetry. Each C/N isotopic combination yields three LVM's, the highest being a C—N stretch mode along the C_1-N axis (indicated schematically by ω_1 in Fig. 6) and the second a C_1 stretch mode with its two carbon neighbors (ω_2 in Fig. 6). The lowest is a N—C stretch mode (ω_3 in Fig. 6) and its frequency is in reasonable agreement with the location of the *H*1*a* band. Although the N atom is bonded to three rather than two C atoms, ω_3 is very weakly coupled to C_1, shifting by $<1\ \text{cm}^{-1}$ with the C_1 mass. Indeed, ω_3 splits into three bands in a ratio of 1:2:1 with an equal $^{13}\text{C}/^{12}\text{C}$ mixture, with the three peaks split by 13 and $15\ \text{cm}^{-1}$, cf. ~ 12 and $14\ \text{cm}^{-1}$ from experiment. The N-isotope shift is also in agreement with *H*1*a*, being calculated to be $25\ \text{cm}^{-1}$ (cf. $24\ \text{cm}^{-1}$).

A general overestimate in the location of the modes and isotope splittings may occur due to the compressive nature of the fixed volume supercell in the presence of an interstitial atom.[42] Allowing the lattice constant to vary to minimize the total energy dilates the supercell by $\sim 1.7V_{\text{ref}}$ ($V_{\text{ref}}=a_0^3/8$), slightly less than that calculated for I.[42] The LVM's calculated with the relaxed lattice constant are also listed in Table II. The agreement with the *H*1*a* bands is indeed closer. However, we shall show later that this agreement is fortuitous, and that there is a more convincing model.

In the positive (negative) charge state, the LVM's are shifted down (up) by 7, 26, and $46\ \text{cm}^{-1}$ (0, 28, and $21\ \text{cm}^{-1}$) for ω_1, ω_2, and ω_3, respectively. Since the positive charge state is unlikely to be important in N-containing material, a simultaneous assignment of *H*1*a* and $1502\ \text{cm}^{-1}$ to two charge states of $N_{i,\,[001]}$ seems unlikely. Although it remains a possibility that $N_{i,\,[001]}$ is responsible for the $1502\ \text{cm}^{-1}$ band, the agreement is not particularly good, and as with *H*1*a*, we shall propose a different model.

For comparison, the LVM's of the C_2 $N_{i,\,\text{BC}}$ are also listed in Table II (this symmetry being chosen because it yields two equivalent neighbors). Although $N_{i,\,\text{BC}}$ has a mode in reasonable agreement with *H*1*a*, since the $^{14}\text{N}/^{15}\text{N}$ shift is very small (just $3-4\ \text{cm}^{-1}$) this structure can also be discounted on the grounds of vibrational frequency.

4. Discussion

The energy and LVM's show that, in contrast to a previous assignment,[18] $N_{i,\,\text{BC}}$ is not a convincing model for the *H*1*a* defect. Instead, of the forms of N_i, our calculations favor $N_{i,\,[001]}$. The acceptor level and a higher-frequency mode in the negative charge state are broadly consistent with

TABLE II. LVM's for N_i (cm^{-1}) in $^{12}\text{C}/^{14}\text{N}$ material. The H1a ir band is at 1450 cm−1.

	Bulk a_0			Relaxed a_0		
[001] split interstitial	1898	1577	1501	1861	1537	1461
Bond center	2020	1503		1983	1472	

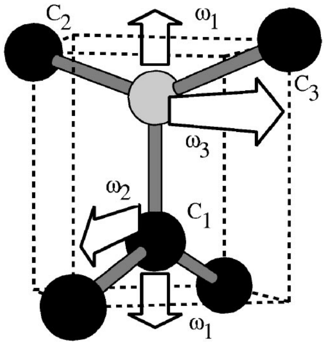

FIG. 6. An illustration of the LVM's of $N_{i,[001]}$. Black and gray circles represent C and N, respectively, the arrows the direction of displacement for the core atoms in each mode, and the dashed lines the cubic axes.

the suggestion that the 1502.0 cm^{-1} band arises from another charge state of the $H1a$ center.[22]

However, a crucial problem remains: the diffusion barrier is too small for the defect to survive to the observed temperatures. If we approximate the hop rate ω_h by

$$\omega_h = \omega_a \exp(-E/k_BT), \quad (3)$$

where ω_a is the attempt frequency, E is the diffusion barrier, k_B is Boltzmann's constant, and T is the absolute temperature, taking $\omega_a = 40$ THz and requiring ω_h to be 1 Hz yield a stability temperature for N_i around 350 °C. Using Eq. (3) with the experimental stability of $H1a$, $T = 1400$ °C, and the calculated diffusion barrier of N_i implies $\omega_a \sim 10^5$ Hz, which seems implausible. Since $T = 1400$ °C and $\omega_a = 40$ THz implies $E \sim 4.5$ eV we conclude that $H1a$ is not due to N_i, but instead due to a more stable interstitial defect.

B. N_i-N_s pair

Theoretically, a pair of N atoms sharing a single site (N_{2i}) constitutes a particularly stable structure in silicon.[43–46] The structure [Fig. 7(a)] possesses D_{2d} symmetry and resembles I and N_i in diamond (Sec. III A). For the relaxed structure, the N—N and N—C bonds are 1.24 and 1.38 Å, respectively, with bond angles of 110° and 139°, close to those of N_i.

N_{2i} is lower in energy than separated, neutral N_i and N_s by 5.1 eV, and 6.9 eV is liberated in the reaction

$$I + A\text{center} \rightarrow N_{2i}.$$

This implies that, as with N_i, once formed, N_{2i} is unlikely to dissociate. Furthermore, it will not form a source of N_i [Eq. (1)] at the temperatures where $H1a$ is stable, contradicting previous propositions.[18]

Metastable partially dissociated structures, similar to those found for N_i (Fig. 2), can also be formed with N_s and N_i, and are shown in Figs. 7(b)–7(f). The DB present in N_s-I defects can be replaced by a nitrogen lone pair. N_i-N_s pairs at second and third neighbors are low in energy in comparison to the dissociated components, and structures (d)–(f) are respectively just 2.9, 1.7, and 2.7 eV higher in energy than the ground-state N_{2i} configuration. N_s neighboring N_i can be achieved with N—N bonds or N_s bonded to the C atom in the split-interstitial [Figs. 7(b) and 7(c), respectively]. These have energies of 3.3 and 3.9 eV, respectively, relative to the ground state. However, in order to convert several of the N_i-N_s structures into N_{2i} an exchange of C and N must take place, and it seems reasonable that there will be a considerable barrier to the formation of the structure in Fig. 7(a) from partially dissociated pairs.

1. Electronic structure

N_{2i} has a donor level around 0.7 eV above the valence-band top (due to N lone pairs) and an acceptor level lying above the conduction band minimum. This is in line with the chemical nature of the defect, with both N atoms being threefold coordinated, and no carbon DB's. The metastable separated pairs also only possess occupied (N-related) orbitals close to the valence-band top. This suggests that N_i-N_s would be electrically, optically, and EPR inactive, with only the atomic vibrations as a mechanism for direct detection of their presence.

2. Migration of N_i-N_s

The path for N_i migration does not apply to N_i-N_s since both N atoms need to move together. Instead, the most probable course is partial dissociation followed by recombination, such as that indicated schematically in Fig. 8. This process includes structures where N_s neighbors N_i. All such structures that we have examined are ⩾3.3 eV higher in energy than that shown in Fig. 1(d). The trajectory in Fig. 8 involves a number of reorientations of N_i, which is likely to

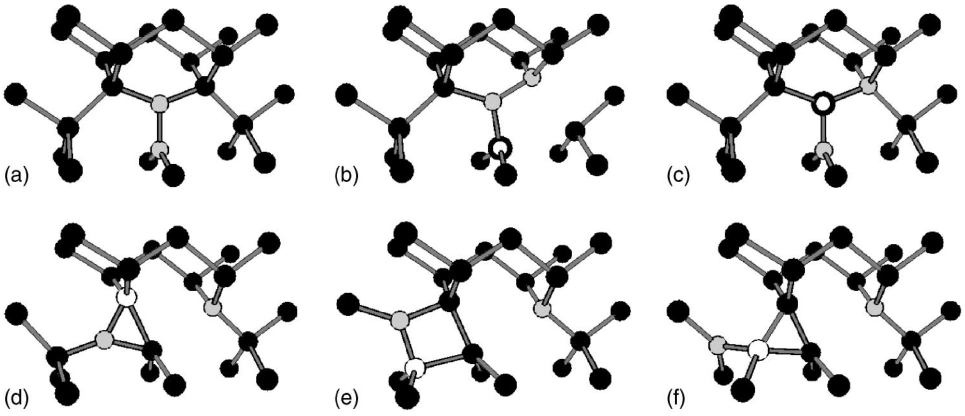

FIG. 7. Schematics of N_i-N_s complexes. (a) [001]-oriented split-interstitial, (b) and (c) nearest-neighbor N_i-N_s, (d) second-neighbor pair, (e) and (f) third-neighbor pairs. Shading and orientation are as defined in Fig. 2.

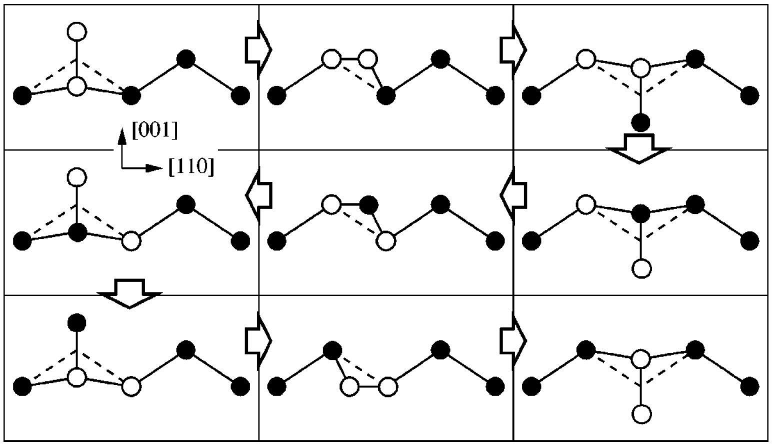

FIG. 8. A possible scheme for the migration of N_i-N_s. Black and gray circles represent C and N, respectively. All atoms plotted are within a single $(1\bar{1}0)$ plane.

involve a barrier of the order of the migration barrier of N_i. Although we have not directly estimated the barrier to migration, the energies of the intermediate structures in Fig. 8 strongly suggests that the activation for the motion of the pair is substantially higher that that of N_i, and broadly consistent with migration around 1400 °C where *H*1*a* is lost.

3. Local vibrational modes

The LVM's for the structure in Fig. 1(d) are listed in Table II. The calculated volume dilation of $1.6V_{\mathrm{ref}}$ is very close to that of N_i. As with $N_{i,\,[001]}$ there are three stretch modes, with ω_2 and ω_3 (Fig. 6), now degenerate, in good agreement with *H*1*a*. In particular, a lack of coupling between the two N atoms in these modes yields *two* rather than three peaks with mixed N isotopes, with the calculated splitting of $23-25\ \mathrm{cm}^{-1}$ encompassing the experimental value of $24\ \mathrm{cm}^{-1}$ for *H*1*a*.[19] The shifts with carbon isotope also agree well with *H*1*a*: 11 and $15\ \mathrm{cm}^{-1}$, cf. 12 and $14\ \mathrm{cm}^{-1}$ from experiment. Therefore, the LVM's of N_{2i} make it a good candidate for *H*1*a*, despite being made up from two N atoms rather than one N atom.

N_{2i} has two equivalent N atoms and the N-N stretch mode is close to the $1856\ \mathrm{cm}^{-1}$ band. However, the N-isotope shifts are in poor agreement with experiment and the different annealing properties of *H*1*a* and $1856\ \mathrm{cm}^{-1}$ centers do not support an assignment of the $1856\ \mathrm{cm}^{-1}$ and *H*1*a* ir bands to the same center. We shall show below that there is a more favorable model for this center.

We have also calculated the LVM's for the partially separated, metastable N_i-N_s pairs (Table III). A N-related mode in the third-neighbor pair lies in reasonable agreement with the $1502\ \mathrm{cm}^{-1}$ ir line, in particular yielding a N-isotope shift of $23-24\ \mathrm{cm}^{-1}$, compared to the experimental value of $25\ \mathrm{cm}^{-1}$. Furthermore, where the three C neighbors to the interstitial-N atom are replaced with ^{13}C, the mode drops by $28\ \mathrm{cm}^{-1}$, in excellent agreement with the $29\ \mathrm{cm}^{-1}$ shift in ^{13}C material.[22] The modes of the second-neighbor pair, and the low-symmetry third-neighbor pair (not listed) are not in particular agreement with any ir bands, and since they are higher in energy than structure (e), Fig. 2, we tentatively correlate the $1502\ \mathrm{cm}^{-1}$ ir band with the third-neighbor metastable N_i-N_s complex.

4. Discussion

The thermal stability and LVM's of N_{2i} are consistent with *H*1*a*. However, such an assignment implies that the formation processes have different activation barriers in Ia and Ib materials, rather than being a charge-state effect. Using the formation temperatures of 300 °C and 650 °C for Ia and Ib material respectively,[18] Eq. (3) yields activation energies of around 1.5 and 2.5 eV.

Noting that in Ia material *H*1*a* is correlated with the concentration of *A* centers,[18] the simplest interpretation is formation of *H*1*a* via $I+A$ center $\rightarrow N_i$-N_s. Assuming that there is no additional barrier to this reaction, this would be activated with an energy appropriate for the migration of the *I*,

TABLE III. LVM's for N_{2i} and the planar second- and third-neighbor N_i-N_s pairs (cm^{-1}). The N isotope for the dissociated pairs refers to that in the split interstitial (see Fig. 7).

Defect	Isotopes	Bulk a_0			Relaxed a_0		
[001] split	^{14}N-^{14}N	1864	1493	1493	1830	1454	1454
	^{15}N-^{14}N	1833	1493	1468	1800	1454	1431
	^{15}N-^{15}N	1801	1468	1468	1768	1431	1431
Second neighbors	^{14}N	2119	1613	1423	2050	1561	1384
	^{15}N	2075	1596	1423	2007	1544	1384
Third neighbors	^{14}N	1833	1552	1443	1774	1501	1402
	^{15}N	1800	1528	1443	1742	1478	1402

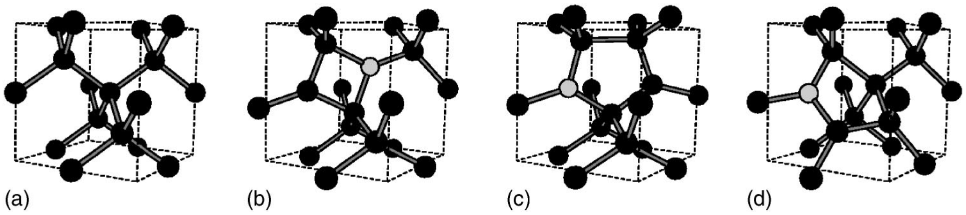

FIG. 9. Schematics of the low-energy forms of N_i-I found in this study. (b), (c) and (d) are analogous to the *R*1, Humble, and π-bonded di-interstitial structures, respectively. Black and gray circles represent C and N atoms. (a) shows a section of defect free diamond for comparison.

consistent with the formation of *H*1*a* in type-Ia material at around 300 °C .

The formation mechanism for N_{2i} in Ib material is less clear. Subsequent to irradiation *I* may complex with N_s and form N_i. Above around 300 °C where we predict N_i is mobile, it should form complexes with other centers in the material, and in particular N_s. However, this direct formation mechanism cannot be correct as *H*1*a* is formed at 650 °C in Ib material, so for the assignment to be correct there must be an intermediate stage in the production of N_{2i}.

Three potential mechanisms suggest themselves.

(1) Under electron irradiation *I* diffuses athermally. During irradiation the dominant form of self-interstitial-nitrogen complex may then involve more than one *I*. The 650 °C threshold would be the mobility of *V* to complex with N_i-I complexes forming mobile N_i, which rapidly forms N_{2i} complexes with N_s.

(2) The migration of N_i may lead to a metastable N_i-N_s complex, which has a barrier to the ultimate formation of the split N-pair corresponding to the 650 °C threshold.

(3) There is a barrier to the formation of N_i from *I* and N_s, so that below 650 °C a metastable form of N_s-I dominates. The annealing step is then the recombination of N_s and *I* into mobile N_i, which migrates to form N_{2i} complexes.

Indeed, our calculations support the formation of both metastable N_s-I and N_i-N_s structures, but it is not possible to be certain based on the present calculations which, if any, of the three mechanisms is correct. However, if an assignment can be made for the 1502 cm^{-1} ir line to the third-neighbor N_i-N_s pair, then this would tend to support the formation of metastable N_i-N_s centers that increases the temperature required for the formation of *H*1*a* in Ib material.

C. N_i-self-interstitial complexes

We have substituted nitrogen for carbon in three low-energy di-self-interstitial structures:[17] the nearest-neighbor pair, correlated with the *R*1 EPR center, the Humble, next-nearest-neighbor structure proposed for the 3*H* optical center, and a π-bonded defect yet to be correlated with any experimental center. Schematics of the complexes are shown in Fig. 9.

In the neutral charge state there is a slight preference for the C_s *R*1 structure. The relative energies are listed in Table IV. In all three cases the nitrogen atom preferentially takes up a threefold-coordinated position, with N_i-I complexes then possessing just one DB. The energy is increased by around 3–4 eV by placing N at a fourfold site consistent with introduction of a second DB.

The binding energies for N_i-I with respect to N_i and *I* are 5.6, 5.8, and 5.2 eV for the positive, neutral, and negative charge states, respectively. These large values correspond to the removal of two DB's, and suggest that these complexes are unlikely to dissociate except at high temperatures.

1. Migration of N_i-I

Since the binding energy is large, the loss of N_i-I would most likely correspond to the further capture of mobile species (such as N_i, *I*, or *V*) or the migration of the complex. A potential migration scheme is portrayed in Fig. 10. This scheme is similar to that proposed for the diffusion of the di-self-interstitial.[17] The intermediate stage with the gray atoms in Fig. 10 has an energy only 0.5 eV above the *R*1 structure. A complete analysis of the motion of N_i-I is computationally expensive, and we are unable to precisely determine the thermal stability of N_i-I. However, it seems reasonable to expect these complexes to be more mobile than N_{2i} since only the N atom is moving through the lattice.

2. Electronic structure

Neutral *R*1 and Humble structures possess one carbon DB, populated by a single electron, whereas the π-bonded model has a partially populated π^* state high in the band gap. Therefore N_i-I is electrically active, the calculated levels be-

TABLE IV. Relative total energies for N_i-I in diamond, and the acceptor and donor levels calculated using the bulk diamond cell as a marker (eV). Acceptor and donor levels are given below the conduction band minimum and above the valence-band top, respectively.

		Charge state				
Model	Symmetry	−1	0	+1	(−/0)	(0/+)
*R*1	C_s	0.0	0.0	0.9	1.2	2.3
Humble	C_s	0.4	0.2	0.9	0.8	2.5
π bonded	C_2	1.7	0.6	0.0	-	3.8

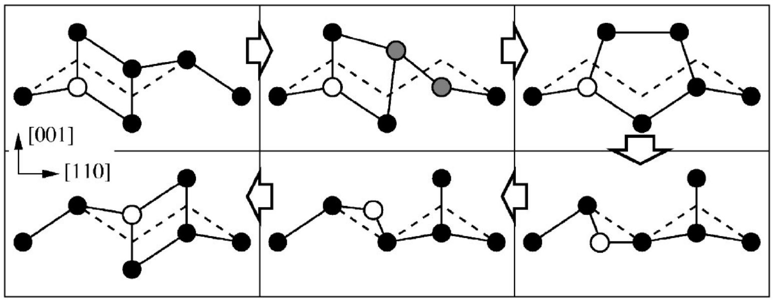

FIG. 10. A possible scheme for the migration of N_i-*I*. Black and white circles represent C and N, respectively. All atoms plotted are within a single $(1\bar{1}0)$ plane, except in the case of the second step where the right-hand split-interstitial (indicated by the gray atoms) is aligned approximately along [010].

ing listed in Table IV. The acceptor levels, lying close the conduction band, means it is unlikely that N_i-*I* will adopt the negative charge state. However, the donor level of the π-bonded structure is above the measured acceptor level of the lattice vacancy [measured at $E_c-2.65$ eV (Ref. 47)].

The location of the Kohn-Sham eigenvalues in the vicinity of the band gap for the three low-energy structures are shown in Fig. 11. As with N_i, the gap has both occupied and empty bands associated with *p* orbitals on N and C atoms. For structures in the positive and neutral charge states these defects represent potentially optically active centers, with excitation energies crudely estimated from the Kohn-Sham levels to lie in the 2–3 eV range, perhaps consistent with the 2.807 and 3.188 eV CL systems.

We also present the Kohn-Sham levels for N_i and *I* separated by two host sites where they are effectively dissociated. The lowest two gap levels reside on the N_i and the nearly degenerate pair higher in the gap are chiefly localized on *I* [cf. Figs. 3(c) and 3(e)]. The $S=3/2$ configuration plotted is calculated to lie around 0.4 eV above an $S=1/2$ ground state. In either spin configuration, this complex is optically active with transitions in the 2–3 eV range, as estimated from the Kohn-Sham levels. It is noted that the *W*11-14 EPR centers seen in irradiated Ib material are of low symmetry and $S=3/2$.[48] These centers are thought to involve N in a passive sense, either as a donor or providing a local strain field. In line with these properties, N_i-*I* complexes in the $S=3/2$ spin state possess spin density chiefly on C atoms, and different separations of the two components might give rise to the range of observations. However, the current model for these centers is a perturbed negative vacancy,[49] and the stability of the EPR centers is not particularly consistent with the migration of self-interstitials.

3. Local vibrational modes

The LVM's for the N_i-*I* complexes are listed in Table V. The low symmetries and relatively large number of atoms involved in these centers complicates the isotopic splittings. However, the modes of the *R*1 structure around 1400–1450 cm^{-1} show very little shift with nitrogen isotope, and can be ruled out as a candidate for the *H*1*a* center.

The 1470 cm^{-1} mode of the Humble structure has a nitrogen isotope shift in agreement with *H*1*a*, and is decoupled from one of its three C neighbors. However the remaining C neighbors are inequivalent, and lead to an isotope pattern with four rather than three peaks at 1470, 1462, 1458, and 1447 cm^{-1}. We can therefore also discount this as a candidate for the *H*1*a* center.

The N-atom in the π-bonded defect has two equivalent C neighbors, and thus might be a candidate for the *H*1*a* defect. However, the modes are rather high in frequency, and the isotopic shifts do not resemble those of *H*1*a*. Therefore we also reject this structure as a candidate for *H*1*a*.

Although there are no obvious links between N_i-*I* complexes and ir bands, all three defects have a relatively large number of LVM's due to the number of inequivalent atoms in strained conditions. Furthermore, given the lack of symmetry, many of these modes may occur as a phonon replica of zero-phonon transitions. This is consistent with the observations of local modes in the side bands of the 2.807 and 3.188 eV CL systems, although it is not possible from the current data to make a firm assignment based on our calculated LVM's.

4. Discussion

Combining the data relating the electrical, optical, and vibrational properties of N_i-*I* defects, we tentatively assign the *R*1 and Humble forms of N_i-*I* to the two CL systems at 2.807 and 3.188 eV. Furthermore, the CL intensity depends upon the exposure to the electron beam, perhaps indicating a change in charge state, consistent with the prediction that N_i-*I* is electrically active.

Since the defects will be optically inactive in the negative charge state, one might suspect that under the electron beam the defects are transformed from negatively charged to neutral. In fact, this is what happens to the vacancy-nitrogen complex in the same material.[26] However, in the case of the vacancy-nitrogen complex, there is a midgap acceptor level, and given that the calculated acceptor levels of N_i-*I* are

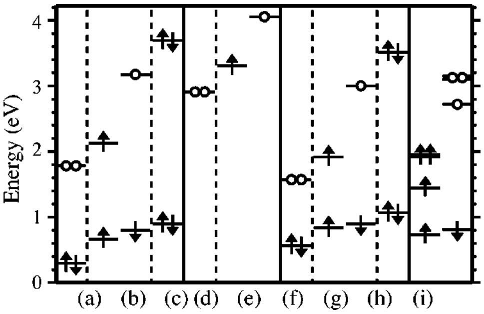

FIG. 11. Kohn-Sham levels in the band gap for N_i-*I* in various charge states. (a)–(c): Humble, +1, 0, and –1; (d) and (e): π bonded, +1, and 0; (f)–(h): *R*1, +1, 0, –1; (i) partially dissociated N_i-*I* pair, made up from $N_{i,[001]}$ and *I* similarly oriented and separated by two host sites. Notation as Fig. 3.

TABLE V. LVM's and isotopic shifts for the N_i-I complexes in diamond (cm^{-1}). Frequencies correspond to N and C masses of 14 and 12 amu, respectively. The ^{15}N shifts represent the reduction in frequency with nitrogen isotope, and the maximum shifts are the reduction in frequency upon replacing all core atoms with ^{15}N and ^{13}C.

Structure								
$R1$	Mode	2032	1833	1642	1603	1445	1433	1417
	^{15}N shifts	2	29	6	18	0	4	0
	Max. shifts	62	51	49	47	26	36	21
Humble	Mode	1817	1769	1564	1470	1428	1399	
	^{15}N shifts	0	30	2	22	0	0	
	Max. shifts	69	63	50	49	23	19	
π	Mode	2023	1933	1782	1575			
	^{15}N shifts	0	39	19	7			
	Max. shifts	79	69	66	58			

higher than the donor level of N_s, such an interpretation seems unlikely. A transition between the neutral and positive charge states remains possible, but it is not obvious why both charge states do not yield optical transitions. Alternatively the enhancement under the electron beam may relate to an increase in the rate at which separated N_i and I combine to form the optical centers, since it is well known the I is highly mobile under ionizing conditions.

D. N_i-N_i complexes

In type-Ia material, *A* centers might capture a pair of self-interstitials to form N_i-N_i complexes analogous to those seen in silicon. Indeed, a defect closely resembling the $R1$ EPR center is the *dominant* form of nitrogen in silicon.[50] As with N_i-I complexes, we have based our analysis on the $R1$, Humble, and π-bonded di-interstitial models. The resulting structures are shown schematically in Fig. 12. The $R1$, Humble, and π-bonded structures have C_{2h}, C_{2v}, and C_{2h} symmetries, respectively, and for all charge states we find $R1$ to be the lowest in energy. The Humble (π) structure is around 0.7 eV (2.4 eV) and 0.5 eV (1.2 eV) higher in energy in the neutral and positive charge state, respectively.

Exchanging a threefold-coordinated N atom for a nearby fourfold site increases the total energy by more than 2 eV, consistent with the formation of a DB. Similarly, separating I and N_{2i} components by two host sites increases the total energy by around 5.3 eV, consistent with the formation of two DB's. In contrast to the partially dissociated N_s-I and N_i-N_s defects, no metastable forms of N_{2i}-I complexes have been found. Thus there is no particular structural reason to suspect a barrier to the formation of N_i-N_i deviating significantly from the migration barriers of I or N_i (~ 1.7 eV).

Table VI lists reaction energies for the formation of N_i-N_i. As with previous complex formation mechanisms, the large binding energy is a consequence of the reduction in the number of DB's and will inhibit dissociation.

1. Migration of N_i-N_i

Potentially, N_i-N_i might migrate in a similar fashion to N_i, as illustrated in Fig. 13. Since the the mechanism is essentially the through-bond diffusion plus the breaking of a reconstructed bond, the barrier is likely to be larger than the 1.7 eV barrier for $N_{i,[001]}$. Indeed, the transition state in Fig. 13 can be viewed as $N_i + N_i$, which corresponds to a considerable increase in energy (Table VI). The migration barrier of N_i-N_i is thus likely to be several eV higher than that of $N_{i,[001]}$, and it is plausible that $N_i - N_i$ would be stable species to high temperatures.

2. Electronic structure

As with N_{2i} all structures (Fig. 12) contain only chemically satisfied species, and hence there are no deep empty levels in the band gap, but the N lone pairs lead to a filled band above the valence-band top. Using the bulk-ionization energy as a reference, the donor levels of the $R1$, Humble, and π-bonded structures lie around $E_v + 1.5$ eV, $E_v + 1.8$ eV, and $E_v + 2.7$ eV, respectively, with no evidence of any acceptor activity. We find no evidence of a second donor level.

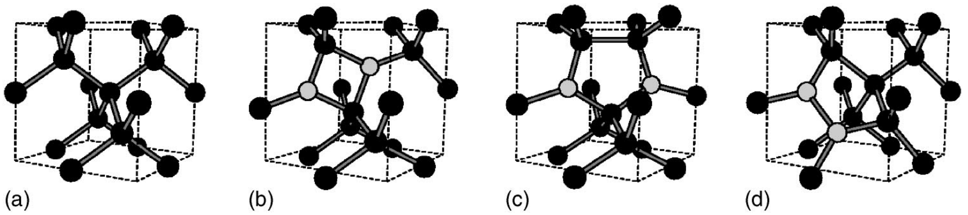

FIG. 12. Schematics of the low energy forms of N_i-N_i found in this study. (b), (c), and (d) are analogous to the $R1$, Humble, and π-bonded di-interstitial structures, respectively. Black and gray circles represent C and N atoms, respectively. (a) shows a section of defect-free diamond for comparison.

TABLE VI. Binding energy E^b (eV) for neutral *I*-nitrogen complexes relative to species likely to be involved in their formation. Unless otherwise stated, the configurations listed refer to the lowest-energy states, and *A* refers to the *A* center.

Reactants	Product	E^b	Reactants	Product	E^b
N_s+I	N_i	5.6	$(N_i\text{-}I)+N_s$	$N_i\text{-}N_i$	5.9
N_s+N_i	N_{2i}	5.1	N_i+N_i	$N_i\text{-}N_i$	6.1
$A+I$	N_{2i}	6.9	$A+I_2$	$N_i\text{-}N_i$	6.2
N_s+I_2	$N_i\text{-}I$	4.2	$(N_{2i})+I$	$N_i\text{-}N_i$	6.6
N_i+I	$N_i\text{-}I$	5.8			
$(N_i\text{-}N_i)+I$	$N_i\text{-}N_i\text{-}I$	6.8	$A+I_4$	$N_i\text{-}N_i\text{-}I_2$	2.6
$A+I_3$(O3)	$N_i\text{-}N_i\text{-}I$	7.1	$(N_i\text{-}N_i)+I_2$	$N_i\text{-}N_i\text{-}I_2$	8.0
$(N_{2i})+I_2$	$N_i\text{-}N_i\text{-}I$	10.4	$(N_i\text{-}N_i\text{-}I)+I$	$N_i\text{-}N_i\text{-}I_2$	8.4

Therefore, it seems most likely that N_i-N_i will be present as a neutral, diamagnetic defect in N-containing material. Furthermore, the presence of only occupied gap states suggests that in the neutral charge state these defects would be optically inactive, and as with N_{2i} they will be most likely detected only by their LVM's.

3. Local vibrational modes

The LVMs of N_i-N_i are listed in Table VII. Of particular interest is the mode at 1917 cm^{-1} for ^{14}N in the *R*1 structure. This ir-active, B_u mode is characterized by displacements of both N atoms approximately along ⟨334⟩. More significantly the two equivalent N atoms yield three peaks in mixed-isotope material, split by 24 and 14 cm^{-1}. Although the frequencies are 3% higher than the experimental values of the 1856 cm^{-1} defect, the isotopic splittings are in very good agreement, and it is tempting to correlate the experimental center with the *R*1 N_i-N_i defect. As with the previous calculations of LVM's, we have also obtained the modes for the *R*1 form of N_i-N_i subsequent to relaxing the volume of the supercell. Focusing on the high-frequency B_u mode, we find that the volume expansion lowers the 1917 cm^{-1} mode to 1845 cm^{-1}, with the nitrogen-isotope splittings being 22 and 14 cm^{-1}, in excellent agreement with the 1856 cm^{-1} experimental data. The only modes in the vicinity of *H*1*a* that exhibit a N-isotope shift are ir inactive, and thus the *R*1 N_i-N_i structure cannot be correlated with this defect.

For the Humble structure a pair of close-by modes lie around 1774 cm^{-1}, made up from odd and even combination of C—N stretches along the split-interstitial bonds. The modes are split by just 2 cm^{-1}, suggestive of a very weak coupling between these oscillators. For mixed nitrogen isotopes there are essentially two frequencies (1774 and 1744 cm^{-1}) split into a number of closely packed modes. Although the overall range of frequencies are consistent with the 1856 cm^{-1} system, the lack of coupling of the two N atoms rules this structure out as a candidate. However, the modes are in close agreement with the 1706 cm^{-1} system, although, as with *H*1*a*, this center is thought to involve only a single N atom. In the volume relaxed system the agreement is excellent, with A_1 modes at 1707 and 1675 cm^{-1} in the ^{14}N and ^{15}N cases. In the mixed isotopes the modes lie at 1678 and 1708 cm^{-1}, and may not be resolved from the isotopically pure cases. There is also an ir-active B_1 mode close by in frequency. However, since this represents an antisymmetric combination of [001] stretch modes, it seems likely that the induced dipole and hence strength of absorption will be small, and may be undetected.

The lack of coupling between the N atoms might allow the Humble structure of N_i-N_i to be responsible for *H*1*a*. However, there is no mode of vibration that yields convincing isotope shifts and as such can also be ruled out as a candidate.

Finally, the π-bonded structure has high-frequency modes that may be related to the 1856 cm^{-1} band. However, the N-related isotopic shifts are not in good agreement and coupled with the relatively high energy of this structure in the neutral charge state, we reject this as a model.

4. Discussion

Complexes made up from two N_s and two *I* form particularly stable structures. Where the N atoms are threefold coordinated, N_i-N_i are chemically satisfied and most probably EPR and optically inactive. The LVM's of the nearest-neighbor pair of *R*1 structure are in very close agreement with the experimental 1856 cm^{-1} band. No other structure examined in this study has two *equivalent* N atoms, modes of the correct frequency with appropriate isotope shifts, and we therefore assign the nearest-neighbor N_i-N_i pair to this experimental system. Additionally, the Humble form has

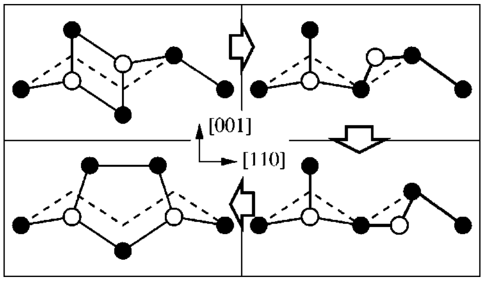

FIG. 13. A possible scheme for the migration of N_i-N_i. Black and gray circles represent C and N, respectively. All atoms plotted are within a single $(1\bar{1}0)$ plane.

TABLE VII. LVM's of N_i-N_i in diamond (cm^{-1}). Symmetries are for isotopically pure cases. For C_{2h} (C_{2v}) symmetry, A_u and B_u (A_1 and B) modes are ir active.

					$R1(C_{2h})$			
N_1	N_2	A_g	B_u	B_u	A_g	A_u	A_g	B_g
14	14	2012	1917	1622	1595	1451	1431	1427
15	14	1994	1894	1615	1584	1451	1426	1427
15	15	1967	1880	1601	1579	1451	1421	1427
					Humble (C_{2v})			
		B_1	A_1	B_1	B_2	A_1	A_2	A_1
14	14	1775	1773	1472	1459	1453	1401	1392
15	14	1773	1745	1465	1459	1440	1401	1389
15	15	1746	1741	1447	1459	1437	1401	1387
					π-bonded (C_{2h})			
		B_g	B_u	A_g	A_u			
14	14	1992	1971	1661	1563			
15	14	1984	1938	1647	1558			
15	15	1948	1932	1631	1554			

LVM's that closely mirror the frequencies and isotopic shifts of the 1706 cm^{-1} precursor to the 1856 cm^{-1} band and is only slightly higher in energy.

It therefore seems plausible that annealing irradiated Ia material leads to a succession of N_i-N_i defects. An anneal of around 900 °C is required for the formation of the 1856 cm^{-1} system, which coincides with the onset of the loss of the 1706 cm^{-1} defect. Assigning the Humble and $R1$ forms to the 1706 and 1856 cm^{-1} centers, respectively, requires a barrier to interconversion of the order of 3 eV, which seems reasonable given the available data.

The 1706 cm^{-1} band appears after annealing to 600 °C, suggesting that the formation of the Humble form of N_i-N_i has a further activation stage. This may relate to the rearrangement of the components of an N_{2i}-I complex, since when initially formed, the N atoms will most likely remain nearest neighbors. The 600 °C threshold (corresponding to an activation energy of ~2.4 eV) would then correspond to a barrier to switch the N atoms from neighboring to the next-nearest-neighbor sites in Fig. 12.

Alternatively, it could be that immediately upon irradiation the dominant form of N-self-interstitial complex contains more self-interstitials, and the lower-temperature annealing threshold is the onset of the motion of lattice vacancies, perhaps involved in a reaction such as A center $+3I+V \rightarrow N_i$-N_i–$I+V \rightarrow N_i$-N_i. Unfortunately, our calculations are unable to resolve which, if either, of these models is correct.

E. Higher-order aggregates

We first examine a potential low energy structure for $2N_s+3I$, which relates closely to the $O3$ EPR center.[6] As before, the N reduces the number of DB's, in this case to zero. The structure is depicted in Fig. 14(b). The reaction energies for the formation of this structure are listed in Table VI. (Theoretically the lowest-energy tri-self-interstitial in diamond is *not* the $O3$ form, but one which is around 1.7 eV lower in energy. However, since this defect does not possess any DB's, there are no obvious sites for N substitution.) Once formed, N_i-N_i-I would be quite stable, since the first reaction in Table VI indicates that the cost of dissociation (estimated by summing the binding energy and I diffusion barrier, 1.7 eV) is 8.5 eV. Thus if N_i-N_i-I is formed in Ia material, the most likely mechanism by which this can be transformed into N_i-N_i, is via the capture of a lattice vacancy. This may correspond to the activation temperature for formation of the 1706 cm^{-1} band.

We have previously examined the possibility of N interacting with tetra-interstitial aggregates in the context of platelets in diamond.[17,51] The lowest-energy structure is shown in Fig. 14(c), and represents a defect with no DB's. However, the tetra-self-interstitial on which this complex is based has no DB's, leading to a relatively small binding energy for the A center to I_4. This and other plausible reactions are listed in Table VI.

The difficulty in forming N_i-N_i-I, N_i-N_i-I_2, and higher-order aggregates relates to the formation path. A centers already present in the material must first trap one I to form N_{2i},

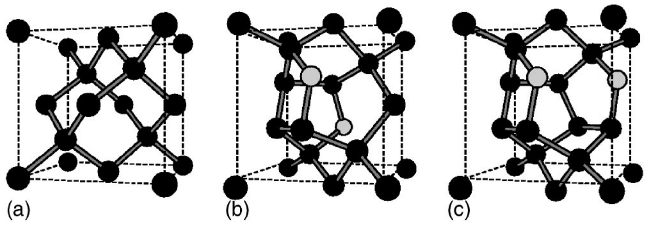

FIG. 14. Schematic representation of (b) N_i-N_i-I and (c) N_i-N_i-$I2$. The black and gray circles represent C and N respectively. (a) shows the corresponding section of defect free diamond for comparison, and the dashed lines indicate the cubic axes.

TABLE VIII. Proposed assignments for N-containing interstitial defects in diamond.

Experimental center	Model
$H1a$ (1450 cm^{-1})	N$_{2i}$
1502 cm^{-1}	N$_i$-N$_s$
1706 cm^{-1}	Humble N$_i$-N$_i$
1856 cm$_{-1}$	R1 N$_i$-N$_i$
2.807 eV and 3.188 eV	R1 and Humble N$_i$-I
2.535 eV and 2.367 eV	dissociated N$_s$-I or N$_i$-I

then a second to form N$_i$-N$_i$ and so on. Purely on statistical grounds the higher-order aggregates would form only for high I concentrations. Furthermore, as the aggregates grow, so do their strain fields, which is likely to further reduce the probability of complex formation. Nevertheless, we note that in IIa material O3 forms at low temperature, albeit in small concentrations, and we cannot exclude the formation of high-order aggregates of self-interstitials and N in type-I material.

1. Electronic structure

Both tri- and tetra-interstitial defects possess filled states close to the valence-band top associated with lone pairs on the N atoms, the tetra-interstitial possessing slightly deeper bands due to the N atoms being closer together. However, they are most likely passive in N-containing material and thus also optically and magnetically inactive.

2. Local vibrational modes

The O3-structure N$_i$-N$_i$-I defect yields several LVM's, the highest two of which are in-phase and antiphase combinations of C—N stretch modes approximately along [001], where both N atoms are the same mass. The antiphase combination is likely to have a much higher ir-absorption coefficient than the in-phase mode, since in the latter case the induced dipoles along [001] cancel. However, in the mixed-isotope case the N—C oscillators become uncoupled and there will be two high-frequency modes. If this defect were present in the material, such ir activity might be interpreted as a defect with *inequivalent* N atoms, although in reality this is not the case.

Where the lattice constant is fixed to the bulk value the modes of N$_i$-N$_i$-I lie at 1441, 1443, 1638, 1726, and 1730 cm^{-1}, all of which are ir active by symmetry. Volume relaxation lowers the frequencies to 1395, 1405, 1577, 1667, and 1671 cm^{-1}. Similar results are obtained for N$_i$-N$_i$-I_2, with around 10 modes above the Raman frequency, the highest lying around 1716 cm^{-1}. However, in neither case is there an obvious experimental system with which to make a correlation.

IV. CONCLUSIONS

Based on the calculated properties of complexes made up from N$_s$ and self-interstitials, Table VIII lists the proposed assignments for radiation products in N-containing diamond. One can then hypothesize the formation paths that are occurring if our assignments are correct.

Ib material. Upon irradiation bound, metastable N$_s$-I complexes are formed that give rise to the optical absorption peaks at 2.367 and 2.535 eV. At moderate temperatures (between around 300 and 650 °C) I becomes mobile and is trapped by some N$_s$-I complexes to form N$_i$-I complexes, giving rise to the 2.807 and 3.188 eV CL peaks. Other N$_s$-I complexes convert into mobile N$_i$, which migrate to form metastable but strongly bound N$_s$-N$_i$ complexes, one of which is responsible for the 1502 cm^{-1} ir system. Upon annealing at and above 650 °C N$_i$-N$_s$ reconstructs to form the D_{2d} symmetry N$_{2i}$ defect, which we correlate with the $H1a$ ir absorption. Above 1400 °C $H1a$ is destroyed. It is not clear by what process this occurs. However, we note that Eq. (3) suggests that 1400 °C corresponds to an activation energy of 4.5 eV, which is considerably lower than the calculated activation barrier to dissociation of 6.8 eV (estimated from the sum of the binding energy and migration barrier of N$_i$). It seems more likely that this threshold either corresponds to the migration of N$_i$-N$_s$, or to that of some other defect that then complexes with the $H1a$ center. This may involve the formation of higher-order complexes that are very stable (compare the binding energies of N$_{2i}$ and N$_i$-N$_i$-I or N$_i$-N$_i$ -I_2, Table VI) and probably immobile. In particular, 1400 °C may relate to a source of I to convert N$_{2i}$ into N$_i$-N$_i$ which we correlate with the 1856 cm^{-1} band, and which is generated in Ib material by annealing to 1400 °C . Alternatively, the 1400 °C threshold may pertain to the breakup of vacancy complexes such as the R10 EPR center, which occurs around this temperature,[52] with N$_{2i}$ being converted into A centers.

Ia material. At around 300 °C self-interstitials move to form complexes with A centers, forming N$_{2i}$, giving rise to $H1a$. Also formed are N$_i$-N$_s$-I pairs, which above around 500–600 °C convert into N$_i$-N$_i$ in both Humble and R1 forms, giving rise to the 1706 cm^{-1} and more stable 1856 cm^{-1} lines, respectively. At higher temperatures (900 °C and above) the Humble form converts into the R1 form. Above 1400 °C the same processes occur to $H1a$ as in Ib material. However, the 1856 cm^{-1} defect persists, consistent with the particularly high binding energy of the R1 N$_i$ -N$_i$ defect.

In summary, we have shown that the currently accepted model for the $H1a$ center in diamond cannot explain the experimental observations. However, a di-nitrogen-interstitial defect appears to have the correct stability and vibrational properties.

This assignment has an important implication for the interpretation of the experimental spectra with mixed isotopes: the interpretation that the presence of two peaks with mixed N isotopes implies one N atom implicitly assumes that all species in the defect couple together in all local modes. With our assignment, the two-peak structure is interpreted as the motion of the nitrogen atoms in the defect are not coupled. This is similar to our interpretation of the 3H optical center, which exhibits a three-peak structure in a phonon replica in mixed carbon isotopes. In this case this is suggestive of two *equivalent* C atoms,[53] but the optical center has been assigned to a defect where two [001]-oriented carbon split-interstitials at next-nearest-neighbor sites oscillate almost independently of each other.[17] The assignment of $H1a$ to an E mode at a D_{2d} N_{2i} defect can be tested experimentally if the symmetry of the vibrational mode can be examined under uniaxial stress.

We are made more confident in our assignment for $H1a$ by how it fits into the broader picture of irradiated N-containing diamond, and the lack of any other system simultaneously possessing vibrational modes and thermal stability consistent with experiment, despite the wide ranging nature of the study. Indeed, by analyzing a range of combinations of N and self-interstitials, we have been able to construct broad schemes for the formation and annealing of defects in Ia and Ib material consistent with the different experimental observations for these materials.

Finally, although we have focused on ir modes that have been correlated with N by isotopic effects, we find many modes in N-containing defects for which there are no N-related isotope shifts. For example, ω_2 in N_i shifts by less than 10^{-2} cm^{-1} with the N mass in our calculations, despite being directly adjacent to the N site. The case is even more clear for defects such as N_i-I and the dissociated N_i-N_s pairs where there are strongly localized modes that are spatially separated from the N site. Many systems such as the 5*RL* optical center are stable to temperatures that perhaps suggest the stabilizing presence of a nearby impurity, and we have shown that defects where N acts as a benign trap are quite plausible.

ACKNOWLEDGMENTS

We would like to thank Professor J. M. Baker and Professor J. W. Steeds for helpful discussions.

---

[1] T. Evans and Z. Qi, Proc. R. Soc. London, Ser. A **381**, 159 (1982).

[2] I. Kiflawi, H. Kanda, D. Fisher, and S. C. Lawson, Diamond Relat. Mater. **6**, 1643 (1997).

[3] A. A. Shiryaev, M. T. Hutchison, K. A. Dembo, A. T. Dembo, K. Iakoubovskii, Yu. A. Klyuev, and A. M. Naletov, Physica B **308-310**, 598 (2001).

[4] A. T. Collins, J. Phys. C **13**, 2641 (1980).

[5] G. Davies, S. C. Lawson, A. T. Collins, A. Mainwood, and S. J. Sharp, Phys. Rev. B **46**, 13 157 (1992).

[6] D. C. Hunt, D. J. Twitchen, M. E. Newton, J. M. Baker, J. K. Kirui, J. A. van Wyk, T. R. Anthony, and W. F. Banholzer, Phys. Rev. B **62**, 6587 (2000).

[7] G. Davies, M. H. Nazaré, and M. F. Hamer, Proc. R. Soc. London, Ser. A **351**, 245 (1976).

[8] Y. Mita, Phys. Rev. B **53**, 11 360 (1996).

[9] J. P. Goss, R. Jones, S. J. Breuer, P. R. Briddon, and S. Öberg, Phys. Rev. Lett. **77**, 3041 (1996).

[10] C. D. Clark, R. W. Ditchburn, and H. B. Byer, Proc. R. Soc. London, Ser. A **237**, 75 (1956).

[11] M. F. Thomaz and G. Davies, Proc. R. Soc. London, Ser. A **362**, 405 (1978).

[12] S. C. Lawson, G. Davies, A. T. Collins, and A. Mainwood, J. Phys.: Condens. Matter **4**, 3439 (1992).

[13] E. S. de Sa and G. Davies, Proc. R. Soc. London, Ser. A **357**, 231 (1977).

[14] R. Jones, V. J. B. Torres, P. R. Briddon, and S. Öberg, Mater. Sci. Forum **143-147**, 45 (1994).

[15] R. Jones, J. P. Goss, P. R. Briddon, and S. Öberg, Phys. Rev. B **56**, R1654 (1997).

[16] D. J. Twitchen, D. C. Hunt, M. E. Newton, J. M. Baker, T. R. Anthony, and W. F. Banholzer, Physica B **273-274**, 628 (1999).

[17] J. P. Goss, B. J. Coomer, R. Jones, T. D. Shaw, P. R. Briddon, M. Rayson, and S. Öberg, Phys. Rev. B **63**, 195208 (2001).

[18] I. Kiflawi, A. Mainwood, H. Kanda, and D. Fisher, Phys. Rev. B **54**, 16 719 (1996).

[19] G. S. Woods and A. T. Collins, J. Phys. C **15**, L949 (1982).

[20] A. Mainwood, Diamond Relat. Mater. **8**, 1560 (1999).

[21] A. Mainwood, Phys. Rev. B **49**, 7934 (1994).

[22] A. T. Collins, G. Davies, H. Kanda, and G. S. Woods, J. Phys. C **21**, 1363 (1988).

[23] A. T. Collins, M. Stanley, and G. S. Woods, J. Phys. D **20**, 969 (1987).

[24] A. T. Collins and G. S. Woods, J. Phys. C **20**, L797 (1987).

[25] A. T. Collins and S. Rafique, Proc. R. Soc. London, Ser. A **367**, 81 (1979).

[26] A. T. Collins and S. C. Lawson, J. Phys.: Condens. Matter **1**, 6929 (1989).

[27] A. A. Gippius, V. S. Vavilov, A. M. Zaitsev, and B. S. Zhakupbekov, Physica B & C **116**, 187 (1983).

[28] S. J. Breuer and P. R. Briddon, Phys. Rev. B **51**, 6984 (1995).

[29] R. Jones and P. R. Briddon, in *Identification of Defects in Semiconductors*, Vol. 51A of *Semiconductors and Semimetals*, edited by M. Stavola (Academic Press, Boston, 1998), Chap. 6.

[30] H. J. Monkhorst and J. D. Pack, Phys. Rev. B **13**, 5188 (1976).

[31] C. Hartwigsen, S. Goedecker, and J. Hutter, Phys. Rev. B **58**, 3641 (1998).

[32] D. A. Liberman, Phys. Rev. B **62**, 6851 (2000).

[33] J.-W. Jeong and A. Oshiyama, Phys. Rev. B **64**, 235204 (2001).

[34] J. P. Goss, P. R. Briddon, S. J. Sque, and R. Jones, Diamond Relat. Mater. **13**, 684 (2004).

[35] D. C. Hunt, D. J. Twitchen, M. E. Newton, J. M. Baker, T. R. Anthony, W. F. Banholzer, and S. S. Vagarali, Phys. Rev. B **61**, 3863 (2000).

[36] Here, we consider N_s to possess a dangling bond on the unique C neighbor.

[37] R. Farrer, Solid State Commun. **7**, 685 (1969).

[38] G. Davies, H. Smith, and H. Kanda, Phys. Rev. B **62**, 1528 (2000).

[39] H. E. Smith, G. Davies, M. E. Newton, and H. Kanda, Physica B **340-342**, 111 (2003).

[40] H. E. Smith, G. Davies, M. E. Newton, and H. Kanda, Phys. Rev. B **69**, 045203 (2004).

[41] P. A. Schultz and J. S. Nelson, Appl. Phys. Lett. **78**, 736 (2001).

[42] J. P. Goss, R. Jones, and P. R. Briddon, Phys. Rev. B **65**, 035203 (2002).

[43] H. Sawada and K. Kawakami, Phys. Rev. B **62**, 1851 (2000).

[44] H. Kageshima, A. Taguchi, and K. Wada, Appl. Phys. Lett. **76**,

3718 (2000).

[45] J. P. Goss, I. Hahn, R. Jones, P. R. Briddon, and S. Öberg, Phys. Rev. B **67**, 045206 (2003).

[46] J. L. McAfee, H. Ren, and S. K. Estreicher, Phys. Rev. B **69**, 165206 (2004).

[47] S. Dannefaer, A. Pu, and D. Kerr, Diamond Relat. Mater. **10**, 2113 (2001).

[48] C. A. J. Ammerlaan, in *Semiconductors*, Landolt-Börnstein, New Series Vol. III22b, edited by O. Madelung (Springer, Berlin, 1998).

[49] J. E. Lowther and J. A. van Wyk, Phys. Rev. B **49**, 11 010 (1994).

[50] R. Jones, S. Öberg, F. Berg Rasmussen, and B. Bech Nielsen, Phys. Rev. Lett. **72**, 1882 (1994).

[51] J. P. Goss, B. J. Coomer, R. Jones, C. J. Fall, P. R. Briddon, and S. Öberg, Phys. Rev. B **67**, 165208 (2003).

[52] K. Iakoubovskii and A. Stesmans, Phys. Rev. B **66**, 045406 (2002).

[53] J. W. Steeds, T. J. Davis, S. J. Charles, J. M. Hayes, and J. E. Butler, Diamond Relat. Mater. **8**, 1847 (1999).